ChemComm

COMMUNICATION

View Article Online
View Journal | View Issue

Cite this: *Chem. Commun.*, 2017, 53, 7748

Received 25th May 2017,
Accepted 16th June 2017

DOI: 10.1039/c7cc04044j

rsc.li/chemcomm

Gram-scale production of nitrogen doped graphene using a 1,3-dipolar organic precursor and its utilisation as a stable, metal free oxygen evolution reaction catalyst†

Mustafa K. Bayazit, *[ab] Savio J. A. Moniz*[b] and Karl S. Coleman [c]

For the first time, a one-step scalable synthesis of a few-layer ~10% nitrogen doped (N-doped) graphene nanosheets (GNSs) from a stable but highly reactive 1,3-dipolar organic precursor is reported. The utilization of these N-doped GNSs as metal-free electrocatalysts for the oxygen evolution reaction (OER) is also demonstrated. This process may open the path for the scalable production of other heteroatom doped GNSs by using the broad library of well-known, stable 1,3-dipolar organic compounds.

Fabrication of nitrogen doped (N-doped) carbon nanomaterials has received significant interest due to their potential application in supports for catalysts, membrane technology, sensors and supercapacitors.[1] Among the N-doped carbon nanomaterials, particular consideration has been given to N-doped graphene nanosheets (N-doped GNSs). For instance, the N-doped GNSs with pyridinic, pyrrolic and/or graphitic N moieties have been demonstrated to display a higher catalytic activity for the oxygen reduction reaction (ORR) compared to commercial Pt/C catalysts in applications such as metal–air batteries and fuel cells.[2] It was also shown that N-doped GNSs are extremely versatile and exhibit high reversible capacity, superior rate capability as well as long-term cycling stability.[1j] However, there are very few reports on their utilization as metal-free electrocatalysts for the oxygen evolution reaction (OER).[3] To date, several synthetic strategies including chemical vapor deposition, arc discharge, and thermal/plasma treatment have been developed to prepare N-doped GNSs with varying elemental nitrogen compositions and environments.[4] These approaches usually require special reaction conditions (*e.g.* plasma, an inert atmosphere, high pressure *etc.*), proceed only at high temperatures (800–1000 °C), and use toxic precursors (*e.g.* chlorinated hydrocarbons, cyanuric chloride *etc.*).[4a] However an environmentally benign precursor, chitosan, has also been demonstrated to yield high-quality single layer N-doped graphene films, although relatively high temperatures between 600 and 800 °C were employed.[5] In order to scale-up the preparation of N-doped GNSs for practical applications, novel, cost effective and less labour-intensive strategies are required. Considering the broad library of well-known 1,3-dipolar organic compounds containing various heteroatoms (*e.g.* nitrogen, sulphur and phosphorus) or their mixtures, 1,3-dipolar cycloaddition polymerization reactions could be utilized as a scalable, low-cost method to synthesize heteroatom containing carbon-based nanostructures. However, to the best of our knowledge no cycloaddition reaction-based synthetic protocol has been reported for the preparation of heteroatom doped graphene or its related structures,[4a,6] although solution-mediated Diels–Alder polymerization,[7] cyclodehydrogenation of bianthryl-based linear polymers[8] and the [2+2] cycloaddition of octafunctionalized biphenylenes[9] were shown to be successful for the preparation of graphene-like nanostructures.

In our previous work we reported that the self-cycloaddition of an *in situ* prepared pyridinium ylide dipole can yield conjugated fluorescent indolizine structures through the addition of a second ylide to the double-bond of pyridine heterocycles.[10] This was shown to occur at a temperature of 150 °C during the surface modification of single-walled carbon nanotubes (SWCNTs). The formation of free indolizine in the absence of an additional reactant revealed that the double bonds in the aromatic ring could act as reactive dipolarophiles under suitable reaction conditions. This phenomenon can be extended in order to synthesize conjugated heterocyclic systems and high molecular weight polymers under suitable reaction conditions, for example, the [2+2] cycloaddition polymerisation of alkenes.[11] In this respect, phthalazinium-1-olates can be used as versatile precursors due to their high reactivity and stability in air.[12] For example, 3-phenyl-phthalazinium-1-olate can be readily prepared under ambient conditions with high yields using phthalic anhydride and phenyl hydrazine derivatives, and can be stored for long periods without decomposition.[13] The reactivity and stability of phthalazinium-1-olates towards conjugated double-bonds were previously demonstrated under

[a] *Department of Chemistry, Imperial College London, London SW7 2AZ, UK. E-mail: m.bayazit@imperial.ac.uk*
[b] *Department of Chemical Engineering, University College London, Torrington Place, London, WC1E 7JE, UK. E-mail: s.moniz@ucl.ac.uk*
[c] *Department of Chemistry, Durham University, South Road, Durham DH1 3LE, UK*

† Electronic supplementary information (ESI) available: TEM, AFM of N-doped GNSs, TGA of N-doped GNSs, C 1s and O 1s XPS and FTIR spectra of N-doped GNSs and electrochemical stability of N-doped GNSs. See DOI: 10.1039/c7cc04044j

solvent-free conditions (220 °C) to introduce nitrogen rich phenylphthalazine groups on the SWCNT surface *via* a 1,3-dipolar cycloaddition pathway.[14]

Herein, we report the first example of the utilization of 1,3-dipolar cycloaddition reactions to fabricate gram-scale N-doped GNSs using a nitrogen rich 1,3-dipole, namely 3-phenylphthalazinium-1-olate, as the only precursor *via* a mild thermal treatment in air. The N-doped GNSs were used as a stable, metal-free catalyst for the electrocatalytic oxygen evolution reaction (OER). In a typical procedure, 3-phenyl-phthalazinium-1-olate containing approximately 12% nitrogen (at%) is carbonized at 480 °C in air to yield N-doped GNSs (Scheme 1). Similar to the previous studies,[10,11] N-doped GNSs are believed to be formed following the successive 1,3-dipolar cycloaddition of 3-phenyl-phthalazinium-1-olate to the reactive double-bonds present on an electron deficient fused benzene ring at relatively high temperatures, as shown in Scheme 1. Raman spectroscopy has been used extensively to study graphitic materials, with the D-band at *ca.* 1350 cm^{-1} linked to the sp^3-type surface defects and can be easily compared to the tangential band (G-band) at *ca.* 1580 cm^{-1}.[15] The Raman spectrum (632.8 nm excitation, 1.96 eV) of the produced carbonaceous material is shown in Fig. 1a, which confirms the formation of a graphitic material. The N-doped GNSs showed an I_D/I_G ratio of 0.68, attributed to the disruption of the graphitic framework in comparison to a non-defective graphite surface.[15] However this ratio was smaller than that of the previously synthesized N-doped graphene structures which exhibited an I_D/I_G ratio in the range of 0.86 to 0.98 for different N-doping levels (10.1–5.6 N%).[16] These findings suggest that the N-doped GNSs produced *via* the 1,3-dipolar self-cycloaddition polymerisation route contain less sp^3-type defects. In fact, surface functionalization of N-doped GNSs, which leads to an increase in the I_D/I_G ratio, is mainly expected as a result of our synthetic method since the reaction proceeds *via* a 1,3-dipolar cycloaddition to the double-bonds on the surface. Less sp^3 defects are sought-after as highly defective N-doped GNSs suffer from reduced electron transport on the surface which can limit their catalytic performance.[4a] Thus less defective N-doped GNSs produced by our 1,3-dipolar self-cycloaddition polymerisation route may be beneficial for catalytic reactions such as ORR/OER since their electron mobility will be improved. In addition, the characteristic 2D-band is observed around 2640 cm^{-1} which is in good agreement with the previously reported few-layer GNSs.[15] The structure of the as-produced N-doped GNSs was further studied by X-ray diffraction, which exhibited a broad [002] reflection at 2θ of 21.46°, corresponding to a *d*-spacing of 0.41 nm (Fig. 1b). This increased interlayer spacing, compared to that of pure graphite (0.37 nm), can be attributed to the introduction of surface groups such as nitrogen containing 5-membered heterocycles into the 2D carbon framework. The other peak at 2θ of *ca.* 44.65° corresponds to the [100] in-plane hexagonal atomic arrangement. Transmission electron microscopy (TEM) images show the presence of a 2D, layered carbon nanomaterial (Fig. 1c). The presence of partially transparent sheets suggests that N-doped GNSs can be exfoliated in amidic organic solvents (*e.g.* NMP and DMF) which has been shown to be effective for the exfoliation of carbon nanomaterials.[17] The TEM image of the N-doped GNSs exhibits some characteristics associated with the formation of slightly twisted GNSs, which might be related to the regioselectivity of the cycloaddition polymerisation process, possibly occurring perpendicular to the plane of the 1,3-dipole (see Scheme 1). Further TEM analysis suggests the formation of 3D-network like layered structures (see the ESI,† Fig. S1). Upon further inspection, the selected area electron diffraction (SAED) pattern displays a ring-shaped pattern with several diffraction spots, due to the stacking of crystalline

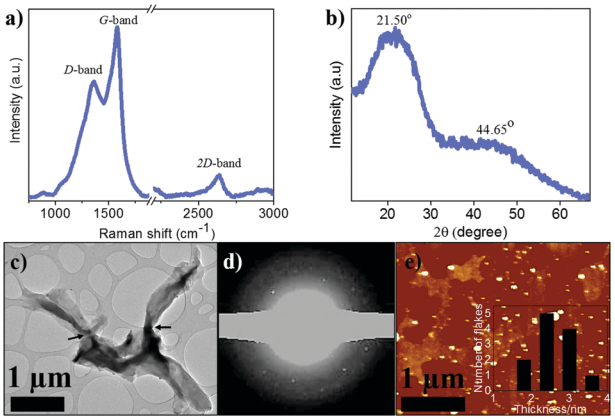

Fig. 1 (a) Raman spectrum of the as-produced N-doped GNSs. (b) XRD pattern of the as-produced N-doped GNSs. (c) TEM image of the N-doped GNS dispersed in NMP. The black arrows show the twisted regions. (d) The selected area electron diffraction (SAED). (e) AFM image with the inset showing the average thickness of the N-doped GNS dispersed in NMP.

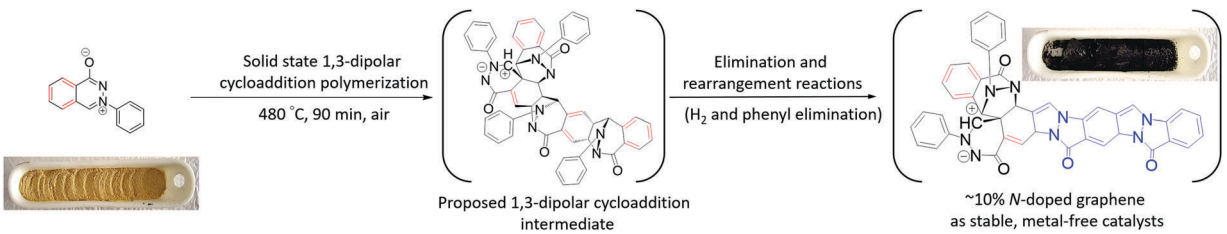

Scheme 1 Formation of N-doped graphene nanosheets *via* a 1,3-dipolar self-cycloaddition of 3-phenyl-phthalazinium-1-olate. The possible 1,3-dipole/dipolarophile interactions are anticipated to take place on the electron deficient fused benzene ring, in which the double bonds are highlighted in red on both the 3-phenyl-phthalazinium-1-olate and the likely intermediate structure. Note that the decomposition of both the precursor and oligomeric carbonized products is also expected at 480 °C in air. The blue region shows the possible planar structure. The orange and black materials in the ceramic boats are 3-phenyl-phthalazinium-1-olate and the resultant N-doped graphene, respectively.

graphitic layers with different angles (Fig. 1d).[18] The AFM height image and the thickness distribution reveal the emergence of N-doped GNSs with lateral dimensions of ~0.5–3 μm and approximately 2.5 ± 0.5 nm in thickness (Fig. 1e and inset and ESI,† Fig. S2). The FT-IR spectrum of the N-doped GNSs shows a sharp peak at 1595 cm^{-1} which is attributed to the C–C stretching bands present in the graphene framework (see the ESI,† Fig. S3). No obvious C═O stretchings were present in the 1650 to 1800 cm^{-1} range except a small shoulder at 1657 cm^{-1} which is due to the formation of a 6-membered lactam ring followed by cycloaddition polymerization. Thus the enhanced D-band in the Raman spectrum of N-doped GNSs may also be correlated with edge effects rather than purely chemical defects.[19] X-ray photoelectron spectroscopy (XPS) was employed to study the elemental composition of the obtained N-doped GNSs. As expected, the XPS survey spectrum of N-doped GNSs shows the presence of C, O and N atoms in 73.18, 17.18 and 9.64 atomic per cent (at%) ratios respectively (Fig. 2a). The percentage of atomic nitrogen in the N-doped GNSs (9.64%) was comparable to that of the 1,3-dipole precursor (11.74%), which indicates almost complete retention of nitrogen atoms after polymerisation. This correlation provides additional evidence that the N-doped GNSs are formed *via* a 1,3-dipolar self-cycloaddition polymerization, rather than a thermal decomposition of the dipole structure at high temperatures. However, it is worth noting that the percentage of oxygen in N-doped GNSs was higher than that of the 1,3-dipole precursor, which suggests surface oxidation (*e.g.* oxides) in air. Fig. 2b shows the deconvoluted N 1s XPS spectra of N-doped GNSs which were fitted by two peaks; they can be attributed to pyrrolic nitrogen (*ca.* 400.2 eV) and pyridinic nitrogen (398.7 eV) with 62.3% and 37.7% contributions, respectively.[4a,20] Obtaining pyrrolic nitrogen-rich N-doped GNSs is not surprising since the 1,3-dipolar cycloaddition of 3-phenyl-phthalazinium-1-olate mainly yields 5-membered pyrazole-type ring structures which confirms the previously proposed reaction pathway. Furthermore, the deconvoluted C 1s XPS spectrum of the N-doped GNSs exhibits three peaks at *ca.* 284.7, 285.9 and 288.9 eV, ascribed to sp^2 carbon with C═C bonds (70.57%), C═N bonds (20.81%) and the physisorbed oxygen (8.62%), respectively, consistent with previous reports (see the ESI,† Fig. S4).[16,21] The thermal stability of the synthesised N-doped GNSs was studied by thermogravimetric analysis (TGA) in both air and helium (see the ESI,† Fig. S5). The TGA curve indicates that the N-doped GNSs decompose at *ca.* 545 °C, similar to graphene (500–600 °C),[22] indicative of good thermal stability.[23] Consistent with the evolution of nitrogen functionalities in carbonaceous materials during pyrolysis,[24] N-doped GNSs exhibited only 25% weight loss at *ca.* 900 °C in air, which may be linked to the formation of stable quaternary nitrogen moieties during TGA that restricts N-oxide formation and subsequent decomposition of the material. Furthermore, a similar weight loss, attributed to covalently-attached surface groups and physisorbed oxygen, was observed at *ca.* 900 °C in helium as well (see the ESI,† Fig. S5). The greater rate of weight loss in helium suggests that the formation of quaternary nitrogen moieties is slower than that in air.

To evaluate the electrocatalytic activities of N-doped GNSs, we chose to investigate their activity towards the oxygen evolution reaction (OER), which has recently been the focus of much attention.[3b] We deposited N-doped GNSs onto both inert carbon paper and nickel foam substrates *via* a simple drop-casting method using Nafion as a binder (see the Experimental section for further details) and tested them in 1 M KOH solution (pH 14). RuO_2 on the nickel foam was used for comparison. Compared to the uncoated carbon paper, the onset of OER in the N-doped GNS was found at approximately 1.5 V *vs.* RHE and a current density of *ca.* 55 mA cm^{-2} was achieved at 1.8 V. Similarly, the N-doped GNS coated onto nickel foam showed an onset of 1.4 V *vs.* RHE and achieved a current density of *ca.* 100 mA cm^{-2} at 1.8 V (Fig. 3). Upon the application of potentials above the onset potential, the evolution of bubbles (oxygen) on the N-doped GNS electrode and hydrogen bubbles on the Pt counter electrode was evident. The small redox peak at *ca.* 1.4 V in the N-doped GNS is likely due to some impurities (*e.g.* nickel oxide species) on the nickel foam substrate; the C–V trace from the N-doped GNS electrode is highly reproducible after scanning several times. The OER activity is higher than that obtained for N-doped graphene/SWCNT hybrids (*ca.* 7.5 mA cm^{-2} at 1.6 V *vs.* RHE)[25] but the onset and total current are a little lower than a benchmark, such as RuO_2. Furthermore, the activity is of the order of that obtained for N-doped graphene nanoribbon networks (*ca.* 15 mA cm^{-2} at 1.6 V *vs.* RHE) recently reported, which is not surprising as both of these N-doped graphenes possess electron-withdrawing pyridinic N moieties,

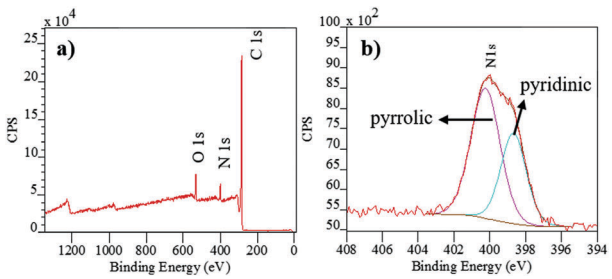

Fig. 2 (a) XPS survey spectrum and (b) N 1s XPS spectrum of the as-produced N-doped GNSs.

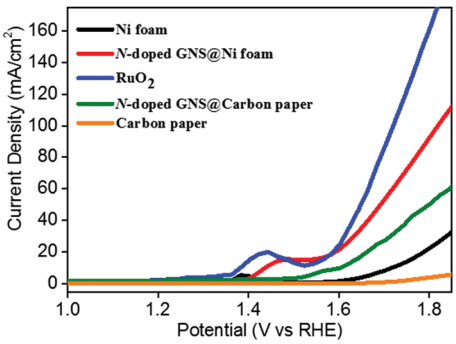

Fig. 3 Current–voltage curves of the N-doped GNS dispersed in DMF and deposited on both carbon paper and nickel foam together with pure carbon paper and nickel foam and RuO_2 on nickel foam for the oxygen evolution reaction (OER), carried out in 1 M KOH (pH 14). The redox peak for RuO_2 is due to the Ru^{V}/Ru^{IV} redox couple.[27]

which can accept electrons (p-type doping) from adjacent C atoms (δ+), facilitating the adsorption of water oxidation intermediates (OH^-, OOH^-).[3] This is effectively the rate-determining step for OER in alkaline solution and thus provides reasoning for the OER activity in N-doped graphenes in contrast to non-doped carbons that exhibit only high conductivity and no appreciable catalytic activity. From DFT studies, the OER active sites have been identified in N-doped graphene nanoribbons at the carbon atoms near the nitrogen atom which possess a minimum theoretical OER overpotential of 0.405 V, which is comparable to Pt-containing catalysts.[26] The electrochemical stability of the N-doped GNS electrodes on both carbon paper and nickel foam substrates was also tested at a fixed overpotential (1.7 V *vs.* RHE) over 24 hours of continued water electrolysis (see the ESI,† Fig. S6). The metal-free N-doped GNS catalyst showed excellent stability with no obvious loss of current under rapid stirring, which was employed in order to force the removal of the accumulated oxygen bubbles from the N-doped GNS surface during water electrolysis. In contrast, RuO_2 displayed inferior stability in KOH, losing over 50% of the activity within the first 10 minutes (see the ESI,† Fig. S7) and is a common observation for Ru-based electrocatalysts under alkaline conditions.[27] Thus the N-doped GNS could be utilised as a low-cost, metal free stable electrocatalyst for OER and potentially as a co-catalyst for photocatalytic water oxidation, the work of which is currently underway.

In summary, for the first time, a 1,3-dipolar cycloaddition reaction was tested and proven to be a suitable synthetic technique for gram-scale production of few-layer 10% N-doped GNSs containing less sp^3-type defects, which was isolated as a stable solid under relatively mild conditions. Photoelectron spectroscopy revealed that N-doped GNSs possessed only pyridinic and pyrrolic nitrogen moieties, the result of a 1,3-dipolar self-cycloaddition polymerisation process which can only produce 6- and 5-membered rings under the aforementioned experimental conditions. The N-doped GNSs exhibited good thermal stability up to 545 °C and yielded approximately 75% carbonized material at 900 °C in air, and could potentially be used in heat resistant coatings and similar applications. Moreover, the utilisation of N-doped GNSs as efficient and stable electrocatalysts for OER has been demonstrated, which opens the path toward their utilisation as metal-free electrocatalysts for the kinetically and thermodynamically challenging process of water oxidation, brought about by the presence of electron-withdrawing pyridinic nitrogen groups. We further anticipate that this scalable high yielding fabrication process for N-doped GNSs will pave the way for the development of other applications that require large amounts of N-doped carbons in order to be low-cost and sustainable. In addition, other heteroatom doped GNSs are expected to be synthesised using the library of well-known 1,3-dipolar organic compounds.

The authors acknowledge funding from EPSRC Grant No. EP/G007314/1 (M. K. B. and K. S. C.) and EU FP7 4G-PHOTOCAT Grant no. 309636 and EPSRC Grant no. EP/N009533/1 (S. M.).

Notes and references

1 (*a*) D. H. Deng, K. S. Novoselov, Q. Fu, N. F. Zheng, Z. Q. Tian and X. H. Bao, *Nat. Nanotechnol.*, 2016, **11**, 218–230; (*b*) C. D. Cress, S. W. Schmucker, A. L. Friedman, P. Dev, J. C. Culbertson, J. W. Lyding and J. T. Robinson, *ACS Nano*, 2016, **10**, 3714–3722; (*c*) W. Cai, C. Wang, X. Fang, L. Yang and X. Chen, *Appl. Phys. Lett.*, 2015, **106**, 253105; (*d*) D. W. Chang and J. B. Baek, *Chem. – Asian J.*, 2016, **11**, 1125–1137; (*e*) L. Feng, L. Yang, Z. Huang, J. Luo, M. Li, D. Wang and Y. Chen, *Sci. Rep.*, 2013, **3**, 3306; (*f*) Y. Liu, L. Yu, C. N. Ong and J. Xie, *Nano Res.*, 2016, **9**, 1983–1993; (*g*) B. Mendoza-Sanchez and Y. Gogotsi, *Adv. Mater.*, 2016, **28**, 6104–6135; (*h*) M. Sevilla and A. B. Fuertes, *ACS Nano*, 2014, **8**, 5069–5078; (*i*) L. Van Nang, N. Van Duy, N. D. Hoa and N. Van Hieu, *J. Electron. Mater.*, 2016, **45**, 839–845; (*j*) Z. Xing, Z. Ju, Y. Zhao, J. Wan, Y. Zhu, Y. Qiang and Y. Qian, *Sci. Rep.*, 2016, **6**, 26146.

2 (*a*) L. Qu, Y. Liu, J.-B. Baek and L. Dai, *ACS Nano*, 2010, **4**, 1321–1326; (*b*) D. Geng, Y. Chen, Y. Chen, Y. Li, R. Li, X. Sun, S. Ye and S. Knights, *Energy Environ. Sci.*, 2011, **4**, 760–764; (*c*) L. Lai, J. R. Potts, D. Zhan, L. Wang, C. K. Poh, C. Tang, H. Gong, Z. Shen, J. Lin and R. S. Ruoff, *Energy Environ. Sci.*, 2012, **5**, 7936–7942.

3 (*a*) H. B. Yang, J. Miao, S.-F. Hung, J. Chen, H. B. Tao, X. Wang, L. Zhang, R. Chen, J. Gao, H. M. Chen, L. Dai and B. Liu, *Sci. Adv.*, 2016, **2**, e1501122; (*b*) D. Guo, R. Shibuya, C. Akiba, S. Saji, T. Kondo and J. Nakamura, *Science*, 2016, **351**, 361–365.

4 (*a*) H. Wang, T. Maiyalagan and X. Wang, *ACS Catal.*, 2012, **2**, 781–794; (*b*) P. Bhunia, E. Hwang, Y. Yoon, E. Lee, S. Seo and H. Lee, *Chem. – Eur. J.*, 2012, **18**, 12207–12212.

5 A. Primo, P. Atienzar, E. Sanchez, J. M. Delgado and H. Garcia, *Chem. Commun.*, 2012, **48**, 9254–9256.

6 Y. Z. Xue, B. Wu, Q. L. Bao and Y. Q. Liu, *Small*, 2014, **10**, 2975–2991.

7 A. Narita, X. Feng, Y. Hernandez, S. A. Jensen, M. Bonn, H. Yang, I. A. Verzhbitskiy, C. Casiraghi, M. R. Hansen, A. H. R. Koch, G. Fytas, O. Ivasenko, B. Li, K. S. Mali, T. Balandina, S. Mahesh, S. De Feyter and K. Müllen, *Nat. Chem.*, 2014, **6**, 126–132.

8 J. Cai, P. Ruffieux, R. Jaafar, M. Bieri, T. Braun, S. Blankenburg, M. Muoth, A. P. Seitsonen, M. Saleh, X. Feng, K. Mullen and R. Fasel, *Nature*, 2010, **466**, 470–473.

9 F. Schlutter, T. Nishiuchi, V. Enkelmann and K. Mullen, *Angew. Chem., Int. Ed.*, 2014, **53**, 1538–1542.

10 M. K. Bayazit and K. S. Coleman, *J. Am. Chem. Soc.*, 2009, **131**, 10670–10676.

11 C. Avendano and A. Briceno, *CrystEngComm*, 2009, **11**, 408–411.

12 C. Najera, J. M. Sansano and M. Yus, *Org. Biomol. Chem.*, 2015, **13**, 8596–8636.

13 (*a*) A. Bongers, I. Ranasinghe, P. Lemire, A. Perozzo, J.-F. Vincent-Rocan and A. M. Beauchemin, *Org. Lett.*, 2016, **18**, 3778–3781; (*b*) N. Dennis, A. R. Katritzky and M. Ramaiah, *J. Chem. Soc., Perkin Trans. 1*, 1976, 2281–2284, DOI: 10.1039/P19760002281.

14 M. K. Bayazit and K. S. Coleman, *Chem. – Asian J.*, 2012, **7**, 2925–2930.

15 A. C. Ferrari and D. M. Basko, *Nat. Nanotechnol.*, 2013, **8**, 235–246.

16 Z.-H. Sheng, L. Shao, J.-J. Chen, W.-J. Bao, F.-B. Wang and X.-H. Xia, *ACS Nano*, 2011, **5**, 4350–4358.

17 H. C. Yau, M. K. Bayazit, J. H. G. Steinke and M. S. P. Shaffer, *Chem. Commun.*, 2015, **51**, 16621–16624.

18 Y.-F. Lu, S.-T. Lo, J.-C. Lin, W. Zhang, J.-Y. Lu, F.-H. Liu, C.-M. Tseng, Y.-H. Lee, C.-T. Liang and L.-J. Li, *ACS Nano*, 2013, **7**, 6522–6532.

19 C. R. Herron, K. S. Coleman, R. S. Edwards and B. G. Mendis, *J. Mater. Chem.*, 2011, **21**, 3378–3383.

20 M. K. Bayazit, L. S. Clarke, K. S. Coleman and N. Clarke, *J. Am. Chem. Soc.*, 2010, **132**, 15814–15819.

21 C. Zhang, L. Fu, N. Liu, M. Liu, Y. Wang and Z. Liu, *Adv. Mater.*, 2011, **23**, 1020–1024.

22 H. Y. Nan, Z. H. Ni, J. Wang, Z. Zafar, Z. X. Shi and Y. Y. Wang, *J. Raman Spectrosc.*, 2013, **44**, 1018–1021.

23 L. S. Panchakarla, K. S. Subrahmanyam, S. K. Saha, A. Govindaraj, H. R. Krishnamurthy, U. V. Waghmare and C. N. R. Rao, *Adv. Mater.*, 2009, **21**, 4726–4730.

24 J. R. Pels, F. Kapteijn, J. A. Moulijn, Q. Zhu and K. M. Thomas, *Carbon*, 1995, **33**, 1641–1653.

25 G.-L. Tian, M.-Q. Zhao, D. Yu, X.-Y. Kong, J.-Q. Huang, Q. Zhang and F. Wei, *Small*, 2014, **10**, 2251–2259.

26 M. Li, L. Zhang, Q. Xu, J. Niu and Z. Xia, *J. Catal.*, 2014, **314**, 66–72.

27 M. Gao, W. Sheng, Z. Zhuang, Q. Fang, S. Gu, J. Jiang and Y. Yan, *J. Am. Chem. Soc.*, 2014, **136**, 7077–7084.